

Lawrence Berkeley National Laboratory

LBL Publications

Title

Fracture Caging to Limit Induced Seismicity

Permalink

<https://escholarship.org/uc/item/8h59n66z>

Journal

Geophysical Research Letters, 48(1)

ISSN

0094-8276

Authors

Frash, LP
Fu, P
Morris, J
[et al.](#)

Publication Date

2021-01-16

DOI

10.1029/2020gl090648

Peer reviewed

1 **Title: Fracture caging to limit induced seismicity**

2 **Authors:** L. P. Frash^{1,2,*}, P. Fu³, J. Morris³, M. Gutierrez², G. Neupane⁴, J. Hampton⁵, N. J.
3 Welch¹, J. W. Carey¹, T. Kneafsey⁶

4 **Affiliations:**

5 ¹Los Alamos National Laboratory, PO Box 1663, Los Alamos, NM 87545, USA

6 ²Colorado School of Mines, 1610 Illinois St, Golden, CO 80401, USA

7 ³Lawrence Livermore National Laboratory, PO Box 808, Livermore, CA 94551, USA

8 ⁴Idaho National Laboratory, 1955 N. Fremont Avenue, Idaho Falls, ID 83415, USA

9 ⁵University of Wisconsin Madison, 1415 Engineering Drive, Madison, WI 53706, USA

10 ⁶Lawrence Berkeley National Laboratory, 1 Cyclotron Road, Berkeley, CA 94720, USA

11 *Correspondence to: lfrash@lanl.gov.

12
13
14

15 **Key Points**

- 16 1. A production well cage can enable high-pressure fluid-injection simultaneously with closed-
17 loop flow-containment in fractured rock.
- 18 2. Model, laboratory, and field evidence indicate that fracture caging can reduce induced
19 seismic magnitudes despite natural complexity.
- 20 3. A cage of production wells improves subsurface flow control and adaptability to transient
21 and dynamic fracture networks.

22 **Abstract**

23 Geothermal resources offer a stable low-carbon energy source. However, geothermal sites can
24 collocate with the hypocenters of large-magnitude seismic events. Large seismic events pose a
25 risk to public safety and are therefore a liability for efforts to develop geothermal resources.
26 Here, we propose ‘fracture caging’ to limit induced seismic event magnitudes and present
27 evidence from numerical model predictions, laboratory experiments, and field observations.
28 Fracture caging involves drilling tactical production wells around a geothermal injection zone to
29 contain fluids in fracture dominated flow systems. Prior to our work, the effect of small wells on
30 the growth of large fractures and on flow through fractures was subject to debate. Our work
31 shows that production wells can impede fracture growth and contain high-pressure fluids in
32 fracture-dominated rocks. This containment offers a mechanism to limit induced seismicity.

33 **Plain Language Summary**

34 Below the ground’s surface, fluid can lubricate rocks which enables them to more easily slip and
35 generate earthquakes. This is a problem for developing geothermal energy resources that require
36 long-term injection of water. If water could be injected without risk of earthquakes, geothermal
37 energy production could be expanded to supply more than 60 GW of electricity in the United
38 States alone. To confront the earthquake risk, we propose that tactical arrangements of
39 production wells around geothermal injection wells can be used to prevent large seismic events.
40 We refer to this arrangement as ‘fracture caging’ because it contains injected fluid in a limited
41 volume of fractured rock in order to prevent uncontrolled stimulation of the larger fractures that
42 generate earthquakes. Prior to this work, we incorrectly assumed that small wells (e.g., 0.3 m
43 diameter) could not inhibit the growth of large fractures (e.g., greater than 100 m diameter). We
44 also incorrectly assumed that these wells could not contain fluids in the dynamic and uncertain

45 fracture networks that are common in natural rocks. However, our models, experiments, and
46 field data now show that fracture caging can work to contain injected fluids and thereby also
47 limit induced seismicity, even in complex natural rock.

48 **Key Words**

49 Earthquake, Geothermal, Risk Mitigation, Energy, Traffic Light Protocol

50 **1. Introduction**

51 In 2017, a 5.4 magnitude injection collocated earthquake rocked Pohang, South Korea, damaging
52 buildings and forcing many residents into emergency housing (Kim et al., 2018; Grigoli et al.
53 2018). Like most geothermal facilities, this site planned for a few injection and production wells
54 to extract heat from the subsurface to generate electricity (Olasolo et al., 2016). This large
55 seismic event occurred despite careful planning and use of ‘cyclic soft stimulation’ to mitigate
56 induced seismicity risk (Hofmann et al., 2019). Unfortunately, this example is just one of many
57 injection-associated seismic events with other notable examples including Basel, Landau,
58 Oklahoma, and Soultz-sous-Forêts (Cuenot et al., 2008; Ellsworth, 2013; Keranen et al., 2013).
59 For Pohang, the damage from the seismic events led to the shutdown of the geothermal plant
60 which had been expected to produce as much as 6.2 MW_e of low-carbon base-load energy.
61 Finding a direct solution to limit induced seismicity is crucial to the future of geothermal energy
62 because earthquakes generated by humans are undesirable, to say the least (Giardini, 2009).

63 Based on a U.S. Department of Energy report (Hamm et al., 2019), an estimated 60 GW_e could
64 be generated by 2050 from the underutilized geothermal resources in the United States alone. At
65 the end of 2015, the total net capacity of geothermal energy production in the United States was
66 only 2.7 GW_e (Geothermal Energy Association, 2016). Currently, the primary seismic risk
67 mitigation strategy is to place geothermal facilities in remote areas, but this greatly limits
68 resource options and increases parasitic energy losses due to long-distance transmission lines. A
69 more ideal solution would be to directly limit induced seismic risk and allow geothermal
70 facilities to be safely located closer to consumers.

71 Building on our recent work (Kneafsey et al., 2019; Frash et al., 2018; Frash et al., 2019; Frash,
72 2020), we now introduce ‘fracture caging’ (Figure 1) as a means to reduce induced seismicity at
73 geothermal sites where flow is dominated by fractures. Fracture caging uses tactical patterns of

74 production wells drilled around injection wells to contain the injected fluids inside of a targeted
75 reservoir. We will show that caging can contain injected fluids by closed-loop flow in otherwise
76 leaky, open, and dynamic fracture systems. Instead of the pressure balancing that is sought by
77 conventional reservoir multi-well solutions (Raleigh et al., 1976), fracture caging uses flow
78 containment to limit the maximum magnitude of seismic events induced by fluid injection or
79 extraction while also enabling safe long-term high-pressure fluid injection. This is a crucial
80 distinction because conventional limits on pressure and flow rates can cripple the energy output
81 potential of geothermal plants but caging imposes lesser restrictions.

82 **2. Fracture Caging Mechanisms**

83 The mechanisms for fracture caging build on four independent constituents: (1) fracture growth
84 is hindered by production wells and leaky fracture networks, (2) fracture flow is contained using
85 a cage of production wells around an injection well, (3) seismic fracture slip is triggered by pore
86 fluid perturbations, and (4) the perturbed length of a fracture has links to maximum seismic event
87 magnitude. Combined, these constituents invoke the ability to limit new fracture growth, contain
88 high-pressure injected fluids within a targeted rock volume, minimize the perturbations in leaky
89 systems that cause shear slip, and thereby limit the number and magnitude of seismic events. In
90 effect, caging induces closed-loop flow inside leaky fracture-dominated flow-networks.

91 **2.1. Fracture growth inhibition**

92 Increasing fracture fluid pressure can induce fracture growth, whether by extension of existing
93 fractures or by creation of new fractures (Valko and Economides, 1995; Rutledge and Phillips,
94 2003; McClure and Horne, 2014). New fracture growth offers a mechanism for seismicity as
95 these fractures grow or when they shear slip (Zhao and Young, 2011). If a growing fracture
96 requiring a high-pressure to propagate intercepts an existing high-permeability feature, such as a
97 well or a large conductive fault, this intercepted feature will act as a pressure sink. However, it is
98 not obvious whether the propagating fracture will be halted, inhibited, or unimpeded by a tiny
99 well of 0.1 to 0.5 m diameter when fractures can exceed 100 m diameter. To investigate this
100 interaction, we employed numerical modeling and laboratory experiments. Interestingly, the
101 results from this work (Figure 2) indicate that production wells can have a profound inhibiting
102 effect on pressure driven fracture propagation.

103 We modeled coupled fracture propagation and fluid flow through a rock and well system using
104 GEOS (Fu et al., 2013; Settgast et al., 2017). For a base case, the rock was assumed to be
105 isotropic, homogeneous, and impermeable granite and the fracture was assumed to be planar.
106 Fracture toughness was included and the injection fluid was water. We evaluated three cases
107 (Figure 2): (1) a single injection well, (2) an injection and production well pair, and (3) a cage of
108 four production wells (producers) around one injection well (injector). Each case was subjected
109 to the same boundary conditions and injection conditions. As expected, the single well model
110 predicted unlimited fracture growth by injection. Partial fracture inhibition in the direction of the
111 producer was predicted in the case of one production well. Fracture inhibition with as much as
112 94% containment of the injected fluid was predicted in the case of the four-producer cage.

113 Laboratory block hydraulic fracture experiments were completed to validate the model's
114 prediction of fracture containment (Figure 2). Here, we show hydraulic fracture geometries
115 created by fluid injection into a granite block (2c), injection and production through another
116 granite block (2f), and within a cage of four production wells in acrylic (2i). The granite natural
117 rock experiments included true-triaxial stress confinement (Frash et al., 2015). Injection of fluid
118 into granite with no production well produced an uncontained fracture through 95% length and
119 100% height of the cubic block. Injection of a larger volume of fluid into the granite block with
120 one production well produced a shorter fracture at 85% length and 50% height of the block. The
121 hydraulic fracture in acrylic was inhibited and contained despite continued injection and nearly
122 imperceptible growth after the fracture intercepted all four of the production wells. The result of
123 containment by four production wells has also been achieved in cement and granite (Frash et al.,
124 2018 and Hu and Ghassemi, 2018), verified by tracers or visual inspection of fractures.

125 Only our most relevant and readily comparable experiments are shown in Figure 2. Additional
126 related experiments have included more heterogeneous materials, different injection parameters,
127 and alternative stress conditions, as performed by others and ourselves (Frash, 2014; Frash et al.,
128 2015; Frash et al., 2018, Hu and Ghassemi, 2018; Frash, 2020). These included shale rocks,
129 cement systems, and other granites. All the multi-well experiments confirmed fracture growth
130 inhibition when the hydraulic fracture intercepted production wells.

131

132 **2.2. Fracture flow containment**

133 Fluid flowing into fractures outside of a targeted injection zone can generate large magnitude
134 induced seismicity (Guglielmi et al., 2015). Furthermore, it has been argued that most high-
135 permeability in-situ fractures and faults are at or near a critical state of stress, where even small
136 perturbations could induce seismic slip (Townsend and Zoback, 2000). However, even in
137 critically stressed fractures, the perturbed portion of large fractures and faults has a controlling
138 effect on induced seismic event magnitudes (Galis et al., 2017). Therefore, flow sinks (i.e.,
139 production wells) around the high-pressure fluid injection zone could prevent fluid flow outside
140 of this zone that would otherwise lead to larger seismic events (Figs. 1 and 2).

141 Parallel-plate experiments were used to model flow containment in permeable open fractures.
142 This represents any large leaky fracture, whether characterized as tensile, shear, or mixed. These
143 used constant-rate injection and production that alternated between red and blue dyed water
144 (Figure 2). The experiments simulated flow from an injection well (2b), an injection-production
145 well pair (2e), and a caged injection well bounded by four equidistant production wells (2h). The
146 injection only scenario was uncontained, the injector-producer pair was partially contained, and
147 the five-well system was nearly completely contained. Tight color band spacing indicates near
148 zero outward flow. This demonstrates that four-well fracture caging in open and permeable
149 fracture systems can contain most injected fluid when the injection rate is equal to production. In
150 the field, tracer surveys and microseismic monitoring can be used to confirm flow containment.

151 **2.3. Fracture and slip criteria in a limited perturbed volume**

152 Many criteria have been developed to model tensile and shear fracture growth, shear slip, and
153 seismicity (Wenzel, 2017; Kang et al., 2019; Morris et al., 1996). For shear fractures, Mohr-
154 Coulomb criteria will predict slip with increasing pore pressure. For tensile fractures, linear-
155 elastic fracture mechanics will predict fracture growth above a critical injection pressure. Shear
156 and tensile fractures interact to form complex networks and wing cracks that are more difficult to
157 analyze. Advanced poromechanical and discrete fracture network models clarify that seismic slip
158 can be induced by pressure increase (injection) or decrease (production), even when fractures do
159 not hydraulically connect back to a well (Segall et al., 1994; Rubinstein and Mahani, 2015;
160 Maxwell et al., 2015). Already, this brief and incomplete description of mechanisms paints a
161 complex picture for predicting seismic fracture growth and slip. However, all these mechanisms

162 originate from a perturbed volume of rock. Fracture caging limits the volume of rock that is
163 perturbed by fluid injection, whether directly or indirectly, and will thereby limit the volume of
164 rock subjected to induced fracture growth and slip.

165 **2.4. Seismic magnitude, perturbed fracture area, and well spacing**

166 A subsurface rupture's length can be related to a maximum event magnitude using the empirical
167 relationship between subsurface rupture length (L_{RLD}) and event magnitude (M_w) established by
168 Wells and Coppersmith (1994), based on a comprehensive collection of field data:

$$169 \quad M_w = 4.38 + 1.49 \cdot \log(L_{RLD}) \quad (1)$$

170 A similar link between seismic magnitude and slip length is established by the definition of
171 seismic moment, M_o (Kanamori and Anderson, 1975). Galis et al. (2017) use numerical models
172 to predict that the inset dimensions of fracture pressure perturbations within large fractures will
173 limit maximum seismic magnitudes, even if the fracture is critically stressed. Thus, the perturbed
174 area of a large fracture is linked to the maximum seismic event magnitude that we could expect
175 from that portion of the fracture. This is the fourth constituent of fracture caging.

176 Established by the four constituent mechanisms above, the perturbed rock volume is defined and
177 controlled by production well placement in a caged system. Thus, the area that is perturbed
178 within large fractures that intersect this volume is also controlled. This volume is most readily
179 defined by the spacing of the wells that form the cage. Therefore, we can postulate that well
180 spacing will link to the maximum magnitude of induced seismic events in a fracture caged
181 system. If true, well spacing substituted for rupture length in Eq. (1) provides a preliminary
182 predictor for the maximum magnitude of seismic events induced in a caged system.

183 **3. Field and Laboratory Fracture Caging**

184 Seismic event cumulative count and maximum magnitude are correlated with cumulative
185 injected fluid volumes (Figure 3). For example, the cumulative number of seismic events
186 measured using a constant detection threshold during injection into the Duvernay shale play is
187 nearly linearly correlated with cumulative injected volumes (Schultz et al., 2018). For another
188 example, maximum event magnitude and cumulative injected volume at various injection sites
189 are also correlated (McGarr, 2014; Galis et al., 2017). However, there are outliers from these
190 trends. One concerning outlier is the large M_w 5.4 event at Pohang. This event is possibly

191 attributed to disturbing a critically stressed fault. In contrast, other outliers exhibited event counts
192 and magnitudes having decaying correlation with injected fluid volume. Data was not adjusted
193 for produced fluid because this adjustment would be victim to speculation. Low seismicity
194 outliers show signs of fracture caging even though they were not optimized for this purpose
195 because caging was not yet considered.

196 One of our granite block laboratory experiments used a 30 cm cubic specimen with one injection
197 well and two production wells (Frash et al., 2015). During this experiment, acoustic emissions
198 peaked early and then decayed despite continued injection to orders of magnitude larger volumes
199 and at faster rates (Figure 3). Corresponding event magnitudes peaked at an injection volume
200 that was less than 1% of the final total injected volume. The granite block's physical size,
201 drained outer boundary, and close well spacing limited the maximum fracture size and limited
202 the maximum possible acoustic emission event magnitude. In effect, this laboratory experiment
203 serves as a near-perfect example of fracture caging reducing induced seismicity.

204 The EGS Collab project (Kneafsey et al., 2019) in Lead, South Dakota, started in 2017 and is
205 ongoing. This project drilled eight 60 m long wells from a 1480 m depth tunnel in schist at the
206 Sanford Underground Research Facility (Figure 4). Water injection created a complex fracture
207 flow network with fracture locations identified by a suite of methods that included microseismic
208 monitoring. Induced seismic events were most prevalent during early high-rate injections and
209 were later observed to decrease despite continued long term injection (Figure 3). This project is
210 an example of a fully caged system because: (1) the injected fluid recovery eventually exceeded
211 95% of the injection rate, (2) seismicity was low after the initial small volume injections, and (3)
212 it was very difficult to inject fluid past the monitoring wells and into the production well.

213 The hot dry rock geothermal project at Hijiori, Japan, lasted from 1985 to 2002 and included four
214 wells with the deepest drilled to a maximum of 2300 m depth in granodiorite (GERD, 1997). The
215 rate of microseismic events was high during the first low-volume injections to stimulate the
216 wells, but the events decreased when production wells were brought online. In fact, seismicity
217 dropped so low during the 1991 circulation tests that the operators decided to do an "AE
218 promotion test" (GERD, 1991) where injection rates were increased by a factor of three to
219 successfully induce microseismicity and confirm that the sensor network was functioning. The
220 trend of renewed induced seismicity and larger induced seismic events due to increased injection

221 rates was consistent through the project to 1995 (GERD, 1995). We lacked access to sufficient
222 data after 1995 for its inclusion in our analysis. This project is a field example of fracture caging
223 with partial containment because recovery of the injected fluid from production wells during
224 circulation tests ranged from 30% to 77%, so some injected fluid was not contained within the
225 targeted stimulated reservoir volume.

226 Production at 100% of the injection rate is not the only factor for reduced seismicity. For
227 example, seismic events greater than M_w 2 were observed during circulation tests at the four-
228 well, 3800 m deep, geothermal site at Soultz-sous-Forêts, France, where operations use 100%
229 reinjection of produced fluids (Cuenot, 2011). In this case, seismic event locations indicate fault
230 activations both away from and between the wells. Also, tracer tests indicated that around 65%
231 of the produced fluid could be natural brine from the surrounding environment (Schill et al.,
232 2017). This indicates that 65% of the high-pressure injected fluid could be leaking away to cause
233 seismicity even though injection and production rates were equal. A complete fracture caged
234 system would be indicated by closer to 100% recovery of injected fluid, perhaps using
235 conservative tracers to confirm a closed-loop system.

236 **4. Challenges from Natural Complexity**

237 Fracture caging to successfully control fluid flow and reduce seismic risk is likely to be sensitive
238 to rock heterogeneity, anisotropy, injection parameters such as fluid viscosity, and general site
239 uncertainty. We investigate complex and dynamic flow through fracture caged systems using
240 laboratory experiments, the highly characterized EGS Collab project, and insights gained from
241 Soultz-sous-Forêts.

242 Modifying the setup from the plate flow experiments in Figure 2, we injected blue-dye into the
243 plate flow model after placing a random distribution of 600 mesh glass beads and air bubbles
244 (Figure 4a,b). Simultaneously, we produced fluid at the same rate from four production wells. In
245 this heterogeneous situation, two production wells became clogged with beads and ceased
246 flowing part way through the experiment. The wells that continued to flow were able to contain
247 the flow in their respective directions despite the added complexity in this experiment. A model
248 with GEOS predicted a similar result by adding stress heterogeneity to the fracture propagation
249 and flow model. These results indicate that more wells are preferable to maximize the likelihood
250 of successful fracture caging.

251 Evidence of transient and dynamically changing flow through a fracture cage was observed by
252 the EGS Collab Project (Kneafsey et al., 2019). Multi-day constant injection-rate tests between
253 October 2018 and April 2019 resulted in erratic flow rates from all the production wells, never
254 reaching a steady state. Initially, water was dominantly produced from the open production well
255 but this changed when a monitoring well (OT) began to produce the most fluid after its cement
256 seal failed. Over time, all wells and the tunnel became production wells. Over 85% recovery of
257 the injected fluid was achieved during the project. The combined well production provided the
258 high recovery and the multiple wells improved adaptability to the dynamic system.

259 We have shown that fracture caging is subject to limitations, but it can still be successful in
260 complex situations. Undesirable situations do exist, such as when fracture network flow bypasses
261 production wells, as was apparent at Soultz-sous-Forêts. Stochastic evaluations that directly
262 consider these scenarios would help optimize well placement to mitigate against complications.
263 Confirmation of caging can be attained by miscroseismic and tracer surveys. Successful caging
264 will depend on confirmation efforts and careful planning that considers complications and
265 anticipates changes to the well system based on the results of the confirmation effort.

266 **5. Conclusions**

267 We offer that fracture caging can mitigate the induced seismicity hazards from high-pressure
268 fluid injection or low-pressure fluid production by arrangements of wells that: (1) inhibit fracture
269 growth, (2) contain pressure perturbations, (3) limit seismic slip lengths, and (4) limit maximum
270 seismic magnitudes. This is akin to creating a closed-loop flow system inside of an open fracture
271 network. Heterogeneity is a challenge for fracture caging that can be overcome by intelligent
272 stochastic design. In addition to limiting seismicity, our models, experiments, and field data
273 analysis indicate that fracture caging can improve fluid containment, increase resilience to
274 dynamic conditions, and enable safe long-term high-pressure fluid injection. While the complete
275 limitations are yet to be determined and more studies may be needed to improve confidence,
276 fracture caging could be a path for increased geothermal energy production at a reduced risk of
277 induced seismic events. It does not escape our notice that fracture caging could have implications
278 beyond geothermal energy, such as for waste disposal wells.

279 **Acknowledgements and Data Availability**

280 **Funding:** This work is supported by Department of Energy (DOE) Basic Energy Sciences under
281 FWP LANLE3W1. The EGS Collab work in this study is supported by the U.S. Department of
282 Energy, Office of Energy Efficiency and Renewable Energy (EERE), Geothermal Technologies
283 Office (GTO) under Contract No. 89233218CNA000001 with Los Alamos National Laboratory,
284 led by Contract No. DEAC02-05CH11231 with Lawrence Berkeley National Laboratory.
285 Research supporting this work took place in whole or in part at the Sanford Underground
286 Research Facility in Lead, South Dakota. The assistance of the Sanford Underground Research
287 Facility and its personnel in providing physical access and general logistical and technical
288 support is gratefully acknowledged.

289 **Author contributions:** Laboratory experiments were conducted and analyzed by L.P.F., J.C.H.,
290 and N.J.W. Data from the EGS Collab site was collected by the EGS Collab team with the values
291 in this manuscript extracted by L.P.F., G.N., and P.F. Numerical modelling with GEOS was
292 performed by P.F. and J.M. Projects making this work possible were led by M.G., J.W.C., and
293 T.K.

294 **Competing interests:** All authors declare no conflicts of interest.

295 **Data and materials availability:** Data for the Hijiori Hot Dry Rock project seismic events was
296 provided by Yanagisawa, N. The EGS Collab project is ongoing with data available on the
297 Geothermal Data Repository (GDR).

298

299

300 **References**

- 301 Cuenot, N., C. Dorbath, L. Dorbath, Induced microseismic activity during recent circulation tests
302 at the EGS site of Soultz-sous-Forêts (France), *Pure and Applied Geophysics* **165**, 797-
303 828 (2008).
- 304 Cuenot, N., F. Michel, D. Catherine, C. Marco, Induced microseismic activity during recent
305 circulation tests at the EGS site of Soultz-sous-Forêts (France), *Proceedings of the*
306 *Thirty-Sixth Workshop on Geothermal Reservoir Engineering* (2011).
- 307 Ellsworth, W.L., Injection-induced earthquakes, *Science* **341**, 1225942 (2013).
- 308 Frash, L.P., *Laboratory-scale study of hydraulic fracturing in heterogeneous media for enhanced*
309 *geothermal systems and general well stimulation*. Colorado School of Mines (2014).
- 310 Frash, L.P, Fracture caging to control earthquake magnitude from induced seismicity: Preventing
311 a repeat of Pohang, *Proceedings of the 54th US Rock Mechanics / Geomechanics*
312 *Symposium* (2020).
- 313 Frash, L.P., K. Arora, Y. Gan, M. Lu, M. Gutierrez, P. Fu, J. Morris, J. Hampton, Laboratory
314 validation of fracture caging for hydraulic fracture control, *Proceedings of the 52nd US*
315 *Rock Mechanics / Geomechanics Symposium* (2018).
- 316 Frash, L.P., M. Gutierrez, J. Hampton, J. Hood, Laboratory simulation of binary and triple well
317 EGS in large granite blocks using AE events for drilling guidance, *Geothermics* **55**, 1-15
318 (2015).
- 319 Frash, L.P., J. P. Morris, EGS Collab Team, Stochastic prediction of multi-well fracture
320 connectivity and application to EGS Collab experiment 2, *Proceedings of the 53rd US*
321 *Rock Mechanics / Geomechanics Symposium* (2019).
- 322 Fu, P., S. M. Johnson, C. R. Carrigan, An explicitly coupled hydro-geomechanical model for
323 simulating hydraulic fracturing in arbitrary discrete fracture networks, *International*
324 *Journal for Numerical and Analytical Methods in Geomechanics* **37**, 2278–2300 (2013).
- 325 Galis, M., J. P. Ampuero, M. Mai, F. Cappa, Induced seismicity provides insight into why
326 earthquake ruptures stop, *Science Advances* **3**, eap7528 (2017).

327 Geothermal Energy Association, 2016 annual U.S. & global geothermal power production
328 report, *Geothermal Energy Association* (2016).

329 GERD. *Summary of Hot Dry Rock Geothermal Power Project in Japan*. (Japan Geothermal
330 Energy Department, 1989, 1991, 1993, 1994, 1995, 1996, & 1997).

331 Giardini, D., Geothermal quake risks must be faced, *Nature* **462**, 848-849 (2009).

332 Grigoli, F., S. Cesca, A.P. Rinaldi, A. Manconi, J.A. Lopez-Comino, J.F. Clinton, R. Westaway,
333 C. Cauzzi, T. Dahm, S. Wiemer, The November 2017 Mw 5.5 Pohang earthquake: A
334 possible case of induced seismicity in South Korea, *Science* **360**, 1003-1006 (2018).

335 Guglielmi, Y., F. Cappa, J.-P. Avouac, P. Henry, D. Elsworth, Seismicity triggered by fluid
336 injection–induced aseismic slip, *Science: Report* **348**, 1224-1226 (2015).

337 Hamm, S. et al., *GeoVision: Harnessing the heat beneath our feet* (U.S. Department of Energy
338 2019).

339 Hofmann, H., G. Zimmermann, M. Farkas, E. Huenges, A. Zang, M. Leonhardt, G. Kwiatek, P.
340 Matrinez-Garzon, M. Bohnhoff, K.-B. Min, P. Fokker, R. Westaway, F. Bethmann, P.
341 Meier, K.S. Yoon, J.W. Choi, T.J. Lee, K.Y. Kim, First field application of cyclic soft
342 stimulation at the Pohang Enhanced Geothermal System site in Korea, *Geophysical*
343 *Journal International* **217**, 926–949 (2019).

344 Hu, L., Ghassemi, A, Lab-scale investigation of a multi well enhanced geothermal reservoir,
345 *Proceedings of the 43rd Workshop on Geothermal Reservoir Engineering* (2018).

346 Kanamori, H., Anderson, D.L. Theoretical basis of some empirical relations in seismology.
347 *Bulletin of the Seismological Society of America* **65**: 1073-1095 (1975)

348 Kang, J.-Q., J.-B. Zhu, J. Zaho. A review of mechanisms of induced earthquakes: from a view of
349 rock mechanics, *Geomechanics and Geophysics for Geo-Energy and Geo-Resources* **6**:
350 171-196 (2019).

351 Keranen, K.M., H. M. Savage, G. A. Abers, E. S. Cochran, Potentially induced earthquakes in
352 Oklahoma, USA: Links between wastewater injection and the 2011 Mw 5.7 earthquake
353 sequence, *Geology* **41**, 699-702 (2013).

354 Kim K.-H., J.-H. Ree, YH Kim, S. Kim, S.Y. Kang, W. Seo, Assessing whether the 2017 M_w 5.4
355 Pohang earthquake in South Korea was an induced event, *Science* **360**, 1007-1009
356 (2018).

357 Kneafsey, T.J., P.F. Dobson, J.B. Ajo-Franklin, et al., EGS Collab Project: status, tests, and data,
358 *Proceedings of the 53rd US Rock Mechanics/Geomechanics Symposium* (2019).

359 Maxwell, S.C., D. Chorney, S.D. Goodfellow, Microseismic geomechanics of hydraulic-fracture
360 networks: Insights into mechanisms of microseismic sources, *The Leading Edge* **34**, 866-
361 984 (2015).

362 McClure, M.W., R. N. Horne, An investigation of stimulation mechanisms in Enhanced
363 Geothermal Systems, *International Journal of rock Mechanics and Mining Sciences* **72**,
364 242-260 (2014).

365 McGarr, A., Maximum magnitude earthquakes induced by fluid injection, *J. Geophys. Res. Solid*
366 *Earth* **119**, 1008-1019 (2014).

367 Morris, A., D. A. Ferrill, D. B. Henderson, Slip-tendency analysis and fault reactivation,
368 *Geology* **24**, 275-278 (1996).

369 Olasolo, P., M. C. Juárez, M. P. Morales, S. D-Amico, I. A. Liarte, Enhanced geothermal
370 systems (EGS): A review, *Renewable and Sustainable Energy Reviews* **56**, 133-144
371 (2016).

372 Raleigh, C.B., J. H. Healy, J. D. Bredehoeft, An experiment in earthquake control at Rangely,
373 Colorado, *Science* **191**, 1230–1237 (1976)

374 Rubinstein, J.L., A. B. Mahani, Myths and facts on wastewater injection, hydraulic fracturing,
375 enhanced oil recovery, and induced seismicity, *Seismological Research Letters* **86**, 1060-
376 1067 (2015).

377 Rutledge, J.T., W. S. Phillips, Hydraulic stimulation of natural fractures as revealed by induced
378 microearthquakes, *Geophysics* **68**, 441-452 (2003).

379 Schill, E., A. Genter, N. Cuenot, T. Kohl, Hydraulic performance history at the Soultz EGS
380 reservoirs from stimulation and long-term circulation tests, *Geothermics* **70**, 110-124
381 (2017).

382 Schultz, R., G. Atkinson, G. W. Eaton, Y. J. Gu, H. Kao, Hydraulic fracturing volume is
383 associated with induced earthquake productivity in the Duvernay play, *Science* **359**, 304-
384 308 (2018).

385 Segall, P., J. R. Grasso, A. Mossop, Poroelastic stressing and induced seismicity near the Lacq
386 gas field, southwestern France, *Journal of Geophysical Research: Solid Earth* **99**, 15423-
387 15438 (1994).

388 Settgest, R.R., P. Fu, S.D.C. Walsh, J.A. White, C. Annavarapu, F.J. Ryerson, A fully coupled
389 method for massively parallel simulation of hydraulically driven fractures in 3-
390 dimensions, *Int. J. Numer. Anal. Methods Geomech.* **41**, 627–653 (2017).

391 Tester, J.W., et al., *The Future of Geothermal Energy: Impact of Enhanced Geothermal Systems*
392 *(EGS) on the United States in the 21st Century* (U. S. Department of Energy 2006).

393 Townsend, J., Zoback, M. D. How faulting keeps the crust strong. *Geology*, 28: 399–402. (2000).

394 Valkó, P., M. Economides, *Hydraulic Fracture Mechanics*, John Wiley & Sons (1995).

395 Wells, D.L., K. J. Coppersmith, New empirical relationships among magnitude, rupture length,
396 rupture width, rupture area, and surface displacement, *Bulletin of the Seismological*
397 *Society of America* **84**, 974-1002 (1994).

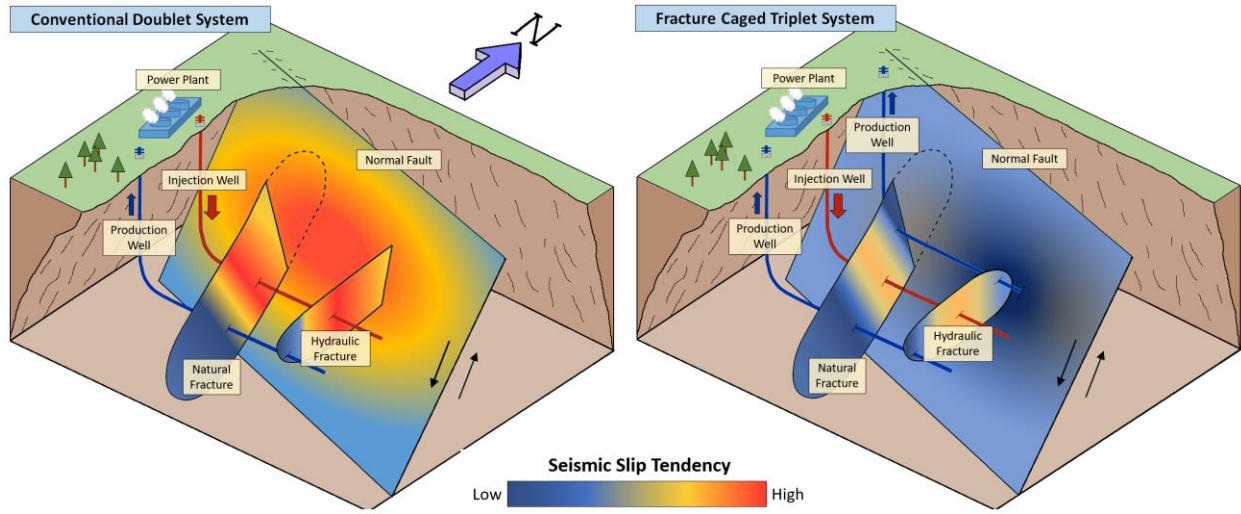
398 Wenzel, F., Fluid-induced seismicity: comparison of rate- and state- and critical pressure theory,
399 *Geothermal Energy* **5** (2017).

400 Zhao, X., R.P. Young, Numerical modeling of seismicity induced by fluid injection in naturally
401 fractured reservoirs, *Geophysics* **76**, WC169-WC182 (2011).

402

403

Figures



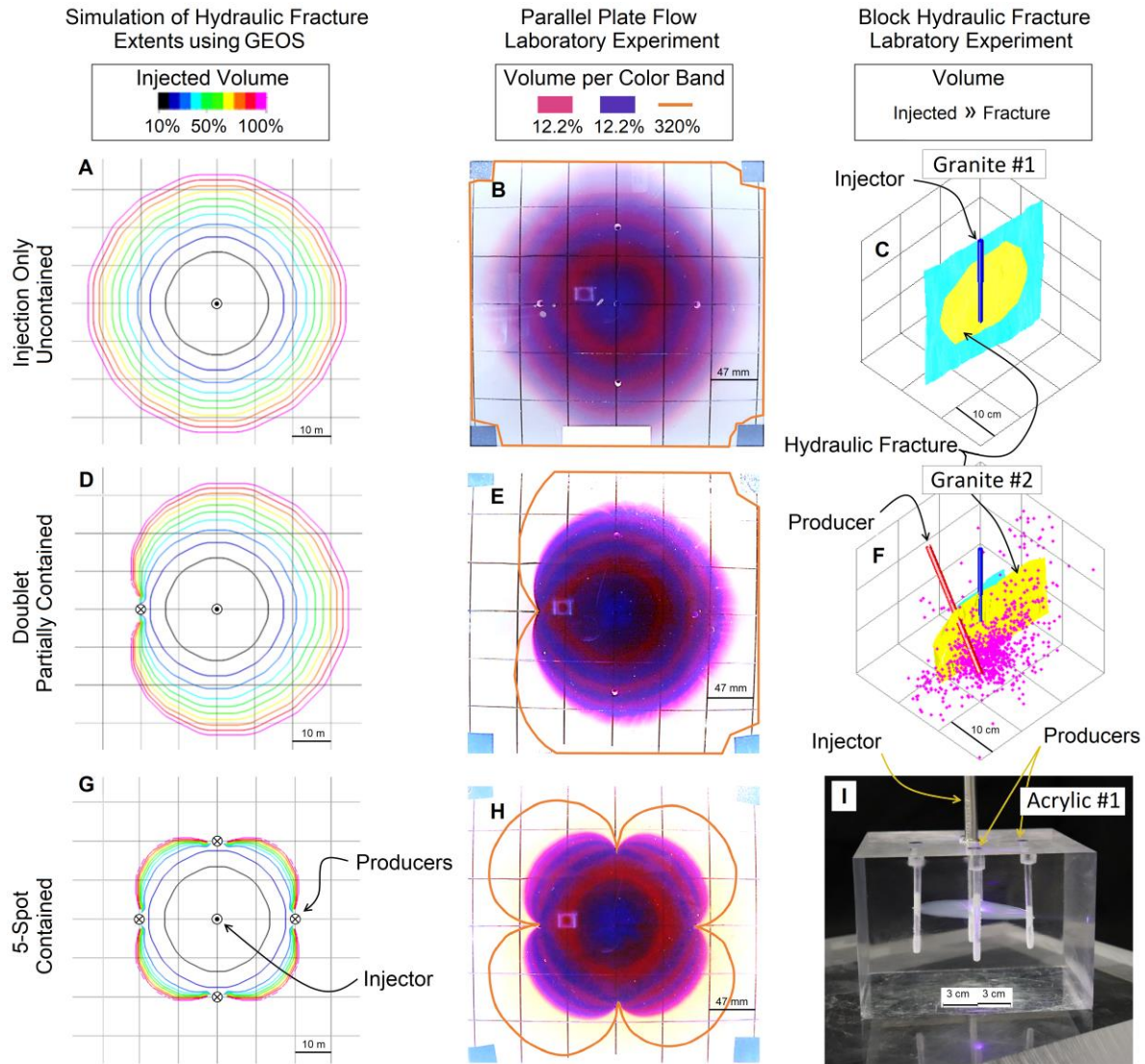
404

405

406

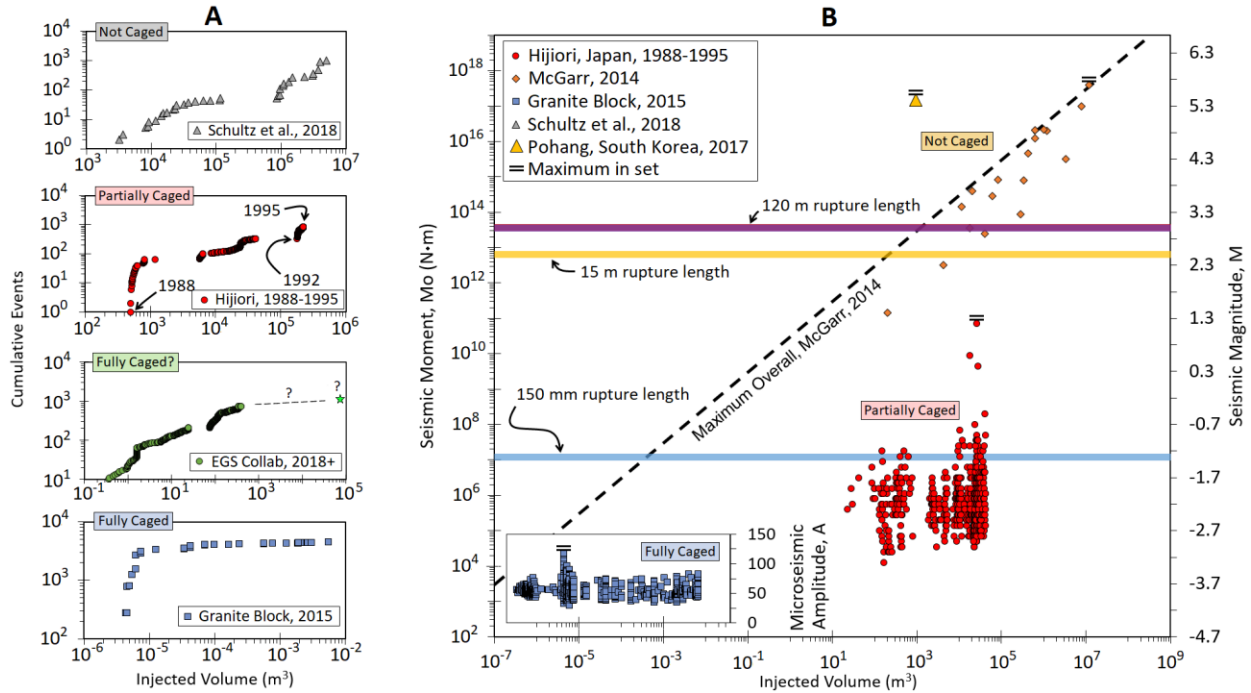
407

Figure 1. Fracture caging to limit seismic slip tendency from geothermal injection wells. The placement of injection and production wells can limit the disturbed volume of rock.



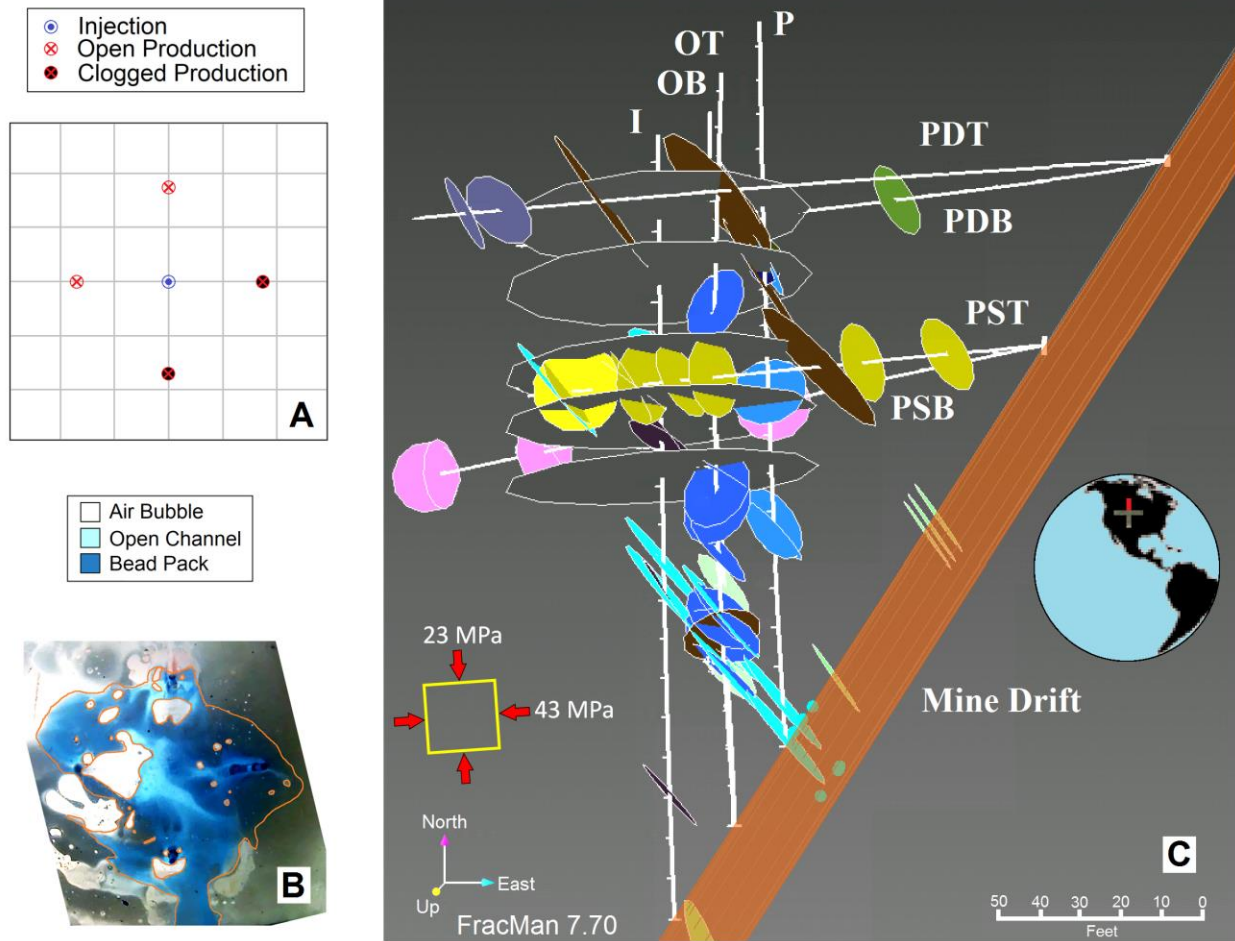
408

409 **Figure 2.** Model and experiments exhibiting fracture caging mechanisms. Fracture growth and
 410 fluid flow are uncontained during injection without production as evidenced by (A) hydraulic
 411 fracture model prediction, (B) parallel plate flow experiments, and (C) cut-sections after
 412 hydraulic fracturing in a granite block. Drilling one production well prior to injection can
 413 partially contain fracture growth and fluid flow during injection as shown by (D) model
 414 prediction for a doublet, (E) parallel plate flow experiments with a doublet, and (F) stimulation
 415 of a doublet in a granite block with acoustic emission hypocenters shown. A 5-spot fracture cage
 416 drilled prior to injection enables containment of fracture growth and fluid flow as found by (G)
 417 model prediction, (H) parallel plate flow experiments, and (I) hydraulic fracturing an acrylic
 418 block.



419

420 **Figure 3.** Induced seismicity behavior with and without fracture caging. **(A)** Cumulative seismic
 421 events plateau with increasing injected volume for fully caged fractures in a laboratory granite
 422 block (Frash et al., 2015) and at the EGS Collab experiment site (Kneafsey et al., 2019) but this
 423 effect is less pronounced in for the leaky partially caged fracture system at the Hijiori Hot Dry
 424 Rock Geothermal Power Project in Japan (GERD, 1997) and almost absent in the injection
 425 dominated Duvernay Shale Play in Canada (Schultz et al., 2018). **(B)** Seismic or acoustic event
 426 magnitudes peak at lower maximum magnitudes as a function of injected volume in the fully
 427 caged laboratory granite block and the partially caged Hijiori project than the peaks observed for
 428 injection dominated systems (McGarr, 2014). Predicted maximum seismic magnitudes (Eq. 1)
 429 for the block experiment, EGS Collab, and Hijiori are shown as a function of the well spacing at
 430 150 mm, 15 m, and 150 m, respectively.



431

432 **Figure 4.** Complexity in fracture dominated flow systems. (A) Glass beads clogging some
 433 production wells and (B) resulting partially caged flow in a heterogeneous parallel plate flow
 434 test. (C) Surveyed layout of EGS Collab Experiment 1 with an injection hole (I), a production
 435 hole (P), six instrumented monitoring holes (OT, OB, PST, PSB, PDT, and PDB), and fractures
 436 that are interpreted to be significant for fluid flow (discs).